Research Square

Preprints are preliminary reports that have not undergone peer review.
They should not be considered conclusive, used to inform clinical practice,
or referenced by the media as validated information.

Hotspot weighted uptake and spatial hotspot descriptors on baseline 18F-FDG PET/CT for risk stratification in NSCLC patients treated with first line chemo immunotherapy

Nitin Gupta

nittinplp@gmail.com

Dr Rajendra Prasad government medical Kangra https://orcid.org/0000-0002-9443-9609

Shipra Sood

Shree Balaji superspecilaity hospital Kangra Himachal Pradesh India

Research Article

Keywords: NSCLC, 18 F-FDG PET/CT, gETU, NHOCmax, NHOPmax, metabolic tumour volume, chemo immunotherapy, prognosis, decision curve analysis

Posted Date: June 5th, 2026

DOI: https://doi.org/10.21203/rs.3.rs-9873079/v1

License: This work is licensed under a Creative Commons Attribution 4.0 International License.
Read Full License

Title Page

Hotspot weighted uptake and spatial hotspot descriptors on baseline ^{18}F-FDG PET/CT for risk stratification in NSCLC patients treated with first line chemo immunotherapy

Running title

FDG PET hotspot weighted uptake in NSCLC chemo immunotherapy

Article type

Original Article

Authors

Nitin Gupta, M.B.B.S., M.D.[1]
Shipra Sood, M.B.B.S., DNB[2]

Affiliations

[1] Department of Nuclear Medicine, Super Speciality Block, Dr Rajendra Prasad Government Medical College, Kangra, Himachal Pradesh, India 176001

[2] [Department of Nuclear Medicine, Shree Balali super speciality hospital, Kangra, Himachal Pradesh, India 176001

Corresponding author

Dr Nitin Gupta, M.B.B.S., M.D.
Department of Nuclear Medicine
Super Speciality Block
Dr Rajendra Prasad Government Medical College
Kangra, Himachal Pradesh, India 176001
Email: Nittinplp@gmail.com
Phone: +91 9882854015

ORCID: 0000-0002-9443-9609

Dr Nitin Gupta:

Keywords

NSCLC; ^{18}F-FDG PET/CT; gETU; NHOCmax; NHOPmax; metabolic tumour volume; chemo immunotherapy; prognosis; decision curve analysis

Funding

No external funding was received for this study.

Conflicts of interest

The authors declare no conflicts of interest related to this work.

Ethics approval

The study was conducted in accordance with the Declaration of Helsinki. Institutional ethics approval and waiver of consent was obtained vide protocol letter no. HFW-H DRPGMC/Ethics/2026/31.

Data availability

De identified data supporting the findings of this study are available from the corresponding author upon reasonable request, subject to institutional and regulatory approvals.

Author contributions

Nitin Gupta: Conceptualization, study design, data analysis, interpretation of results, manuscript drafting, critical revision, and final approval of the manuscript.

Shipra Sood: literature search, manuscript editing and formatting

Acknowledgements

None.

Words in abstract: 297

Words in Manuscript: 1955

Number of tables: Main table 3, supplementary tables: 2

Number of figures: 10

Original research

Hotspot weighted uptake and spatial hotspot descriptors on baseline ^{18}F-FDG PET/CT for risk stratification in NSCLC treated with first line chemo-immunotherapy

Abstract

Background: Baseline ^{18}F-FDG PET/CT provides quantitative information on metabolic tumourr burden in non small cell lung cancer, but the prognostic value of newer hotspot weighted uptake and spatial hotspot descriptors in patients receiving first line chemo immunotherapy remains uncertain.

Aim: To investigate whether hotspot weighted uptake (generalized effective total uptake, gETU) and spatial hotspot descriptors normalized hotspot to centroid distance (NHOCmax) and hotspot to perimeter distance (NHOPmax) add clinically useful

information beyond TNM stage, histopathology, and molecular biomarkers in first line chemo-immunotherapy remains uncertain.

Methods: We analyzed 149 consecutive NSCLC patients treated with first line chemo-immunotherapy. Baseline PET metrics included SUVmax, MTV, TLG, gETU, NHOCmax and NHOPmax. Overall survival (OS) and progression free survival (PFS) were assessed using Cox proportional hazards models. Incremental predictive performance was evaluated by 5 fold cross validated Harrell C-index and 24 month decision curve analysis.

Results: gETU was highly collinear with TLG (Spearman $\rho = 0.999$) and MTV ($\rho = 0.929$), while NHOCmax and NHOPmax were strongly inversely correlated ($\rho = -0.957$) . High gETU (median split) was associated with shorter OS (median 19.0 vs 27.5 months; log-rank $p < 0.001$) and PFS (8.1 vs 14.9 months; $p < 0.001$). In multivariable Cox models adjusting for metastatic stage (IV vs I-III), EGFR status and PD-L1 categories, gETU (per 1 SD) remained independently associated with OS (HR 1.48; $p<0.001$) and PFS (HR 1.51; $p < 0.001$). Adding gETU improved cross validated discrimination for PFS and modestly improved OS, whereas NHOCmax/NHOPmax did not yield consistent incremental gain. Decision curve analysis showed higher net benefit for the gETU augmented model across clinically relevant thresholds.

Conclusion: In this NSCLC chemo-immunotherapy cohort, gETU provides incremental prognostic information beyond TNM stage and molecular biomarkers, while hotspot

location descriptors (NHOCmax/NHOPmax) did not consistently improve prediction once metastatic stage and tumor burden were accounted for.

Keywords

NSCLC; ^{18}F-FDG PET/CT; gETU; NHOCmax; NHOPmax; metabolic tumor volume; chemo-immunotherapy; prognosis; decision curve analysis.

Introduction

Non small cell lung cancer (NSCLC) remains a leading cause of cancer mortality worldwide despite advances in systemic therapy[1]. The introduction of immune checkpoint inhibitors combined with platinum doublet chemotherapy has improved survival in metastatic non squamous and squamous NSCLC and is now a dominant first line strategy[2,3].

Clinical and molecular biomarkers used for treatment selection and risk stratification include TNM stage, histopathology, driver mutations such as EGFR, and tumor PD-L1 expression. However, PD-L1 is an imperfect predictor due to substantial intra and inter-tumoral heterogeneity and sampling effects[4].

Baseline ^{18}F-FDG PET/CT provides quantitative measures of tumor glucose metabolism. Standard semiquantitative metrics include SUVmax, while volumetric measures such as metabolic tumor volume (MTV) and total lesion glycolysis (TLG) capture metabolic tumor burden and have shown prognostic value in NSCLC treated with PD-1/PD-L1 inhibitors

and related regimens[5-8]. Integrating PET derived tumor burden with TNM classification has also been proposed to refine prognostication beyond anatomic staging alone[9].

Beyond conventional tumor burden metrics, Rahmim and colleagues proposed generalized effective total uptake (gETU), a tunable hotspot weighted uptake volume metric designed to better characterize heterogeneous lesions and unify SUVmax and TLG like behavior within a single framework.[10] In parallel, spatial hotspot descriptors such as the normalized distance from the uptake hot spot to the tumor centroid (NHOC) and to the tumor perimeter (NHOP) have been suggested as biologically relevant markers of aggressive phenotypes, reflecting a potential shift of maximal metabolic activity toward the lesion edge during progression[11,12].

Radiomics approaches applied to baseline ^{18}F-FDG PET/CT have also demonstrated associations with checkpoint blockade benefit in advanced NSCLC, supporting the idea that intratumoral heterogeneity can carry clinically actionable information.[13,14] However, it is unclear whether simpler, directly interpretable hotspot weighted uptake (gETU) and hotspot location metrics (NHOCmax/NHOPmax) add clinically useful information beyond TNM stage, histopathology, and molecular biomarkers in patients receiving first line chemo-immunotherapy. We therefore evaluated whether gETU and hotspot location descriptors provide incremental prognostic value over standard PET metrics (SUVmax, MTV, TLG), TNM stage, histopathology, EGFR status, and PD-L1 expression.

Methods

Study design and patients

This retrospective cohort study included 149 consecutive patients with biopsy confirmed NSCLC who underwent baseline ^{18}F-FDG PET/CT prior to first line chemo-immunotherapy between January 2021 to December 2024. Clinical variables and ^{18}F-FDG PET/ CT metrics that were recorded included age, sex, TNM stage, histopathology, EGFR status, PD-L1 expression category (negative/low/high), SUVmax, MTV, TLG< gETU, NHOCmax and NHOPmax respectively.

Imaging, tumor segmentation and PET metrics

PET/CT Acquisition and Image Segmentation

All examinations were acquired on a GE Discovery IQ 610 hybrid PET/CT system (GE Healthcare, Waukesha, WI, USA). Patients received approximately 8-10 mCi of ^{18}F-FDG, and imaging was performed after a standard uptake interval of approximately 60 minutes. Whole body PET emission data were acquired in three dimensional mode, with diagnostic CT using intravenous contrast unless contraindicated. Quantitative image analysis was performed using a Python based workflow. Primary lung tumour volumes of interest were delineated on baseline PET/CT using a standardized semi-automated approach, with contour initialization by Random Walker segmentation followed by manual refinement and consensus review by two experienced nuclear medicine physicians. Organ and nodal exclusion priors generated using Total Segmentator (version 2.12)[13] and nnUNetV2 (version 2.6.4)[14] were used during contour refinement to reduce spill-in from physiologic uptake, nodal disease or adjacent structures when needed (22,23). Random Walker initialization used a bounded primary tumour region on fused PET/CT, foreground seeds placed within the visually confirmed intratumoural FDG avid core, and background seeds

placed in adjacent non tumour tissue and in exclusion masks. No universal hard SUV threshold was used as the final contour rule. Manual editing was limited to correction of obvious non primary tumour uptake, physiologic spill in, skin, chest wall, nodal disease or adjacent organ activity, and all final contours were reviewed in axial, coronal and sagittal planes. Custom Python 3.10 scripts used to compute PET metabolic parameters (SUVmax, MTV, TLG) and spatial hotspot metrics (gETU, NHOPmax, NHOCmax) respectively. Multiplanar visualization of a hypermetabolic lung tumor and its segmentation on baseline ^{18}F-FDG PET/CT are demonstrated in **figure 1.** Derivation of spatial hot spot parameters gETU, NHOPmax and NHOC max are demonstrated in **figure 2.**

Outcomes

Overall survival (OS) and progression free survival (PFS) were analyzed in months. Events were defined by OS Event and PFS Event (1= event, 0 = censored).

Statistical analysis

Statistical analyses were performed in MiniTab version 22.1 (Minitab, LLC, PA, USA), and MedCalc version 23.0.9 (MedCalc Software Ltd, Ostend, Belgium). Ridge regularized sensitivity analyses was carried out with custom python script using python version 3.10. Continuous variables were summarized as median (interquartile range, IQR) and categorical variables as counts (percent). Associations among PET derived metrics were assessed using Spearman correlation (Figure 3). For visualization, patients were dichotomized by median gETU and Kaplan-Meier curves were compared using the log-rank test (Figures 4-5).

Primary inference used Cox proportional hazards models (Breslow method for ties). Because stage I-II counts were small, TNM stage was modeled primarily as a binary term (stage IV vs stages I-III) in multivariable models. Covariates included stage, EGFR status, PD-L1 category (two indicator variables with negative as reference), and standardized gETU (per 1 SD). Results were reported as hazard ratio (HR) with 95% confidence interval (CI) and two sided p values (Tables 2-3; Figures 6-7).

Incremental predictive value was evaluated using 5 fold cross validated Harrell C-index computed on held out folds for OS and PFS models that sequentially added PET metrics to a clinical+molecular baseline model (age, sex, histology, stage, EGFR, PD-L1) (Figures 8-9). Clinical utility for 24 month OS risk was explored with decision curve analysis comparing the baseline clinical+molecular model against a gETU augmented model; patients censored before 24 months were excluded from the decision curve dataset (Figure 10).

Sensitivity analysis

Because categorical stage modeling (I-II/III/IV) led to numerical instability due to near complete event rates in advanced stages, a ridge-regularized Cox model was fit for this grouping and uncertainty was summarized using bootstrap resampling (Supplementary Table S1).

Results

Baseline study cohort characteristics are summarized in Table 1.

PET metric collinearity was substantial, with strong correlations between gETU and TLG ($\rho = 0.999$) and between gETU and MTV ($\rho = 0.929$), while NHOCmax and NHOPmax were strongly inversely correlated ($\rho = -0.957$) (Figure 3).

On Kaplan-Meier analysis, patients with high baseline gETU had shorter OS (median 19.0 vs 27.5 months; log-rank $p < 0.001$) and shorter PFS (8.1 vs 14.9 months; $p<0.001$) (Figures 4-5).

In multivariable Cox models adjusting for metastatic stage, EGFR status and PD-L1 category, gETU (per 1 SD) remained independently associated with both OS and PFS (Tables 2-3). Forest plots of the multivariable models are shown in Figures 6-7.

Cross validated discrimination improved when PET tumor burden metrics (MTV, TLG, or gETU) were added to the clinical+molecular baseline model, with the largest gains observed for PFS (Figures 8-9). Adding NHOCmax or NHOPmax did not yield consistent improvement in held out discrimination.

Decision curve analysis demonstrated higher net benefit for the gETU augmented model over the baseline clinical+molecular model across a range of threshold probabilities for 24 month death risk (Figure 10).

Discussion

In this cohort of NSCLC patients treated with first line chemo-immunotherapy, hotspot weighted uptake (gETU) provided incremental prognostic information beyond TNM stage and molecular biomarkers, whereas hotspot location descriptors (NHOCmax/NHOPmax)

did not consistently improve risk prediction once metastatic stage and metabolic tumor burden were accounted for. Our findings support the broader literature demonstrating that baseline ^{18}F-FDG PET derived metabolic tumor burden is a strong prognostic factor in NSCLC treated with PD-1 inhibitors, including prospective evidence where MTV and TLG were associated with overall survival and early treatment discontinuation[6]. More recent work has further emphasized total metabolic tumor volume as a practical 'game changer' in metastatic NSCLC treated with immunotherapy, reinforcing the central role of baseline burden for outcome stratification[7].

In settings more similar to first line immunotherapy selection, Yamaguchi and colleagues reported that baseline metabolic tumor volume predicted outcomes in PD-L1 ≥50% NSCLC treated with first line pembrolizumab[8]. Our cohort differs in that patients received chemo-immunotherapy across PD-L1 categories, consistent with pivotal phase III trials demonstrating benefit of pembrolizumab-chemotherapy combinations regardless of PD-L1 level in both nonsquamous and squamous metastatic NSCLC[2,3]. This broader treatment landscape may partially explain why PD-L1 category was not a dominant independent prognostic factor in our multivariable models, particularly given known spatial heterogeneity of PD-L1 expression across tumor sites[4].

Although gETU was independently associated with OS and PFS in multivariable analysis, we observed near complete collinearity between gETU and TLG ($\rho = 0.999$), indicating that in this dataset gETU largely behaves as a tumor burden surrogate rather than a distinct heterogeneity marker. This is compatible with the original gETU framework proposed by Rahmim et al., in which gETU spans a family of uptake volume summaries and can approximate TLG like behavior depending on the chosen exponent and implementation[10].

Practically, this implies that gETU may be best interpreted as an alternative burden weighted metric that can be tuned to increase hotspot emphasis, and future work should evaluate exponent selection and standardization across scanners to maximize incremental value[10].

By contrast, hotspot location descriptors (NHOC/NHOP) did not add consistent value beyond stage and burden like PET metrics in our cohort. Recent studies have suggested that NHOC/NHOP reflect biologically meaningful 'edge-shift' of maximal uptake and can predict adverse outcomes in other contexts; for example, Hong et al. linked normalized hotspot distances to response in breast cancer, providing a mechanistic rationale for these features as aggressiveness markers[11]. In lung adenocarcinoma, Zheng et al[12] reported that NHOC and NHOP predicted recurrence and disease free survival after surgery. The discrepancy with our findings may relate to differences in disease stage (advanced systemic therapy vs operable disease), tumor segmentation conventions, and the dominance of whole body burden effects in metastatic cohorts, where the global extent of disease may overwhelm within lesion hotspot spatial variation.

Radiomics studies further underscore that heterogeneity features can be predictive of checkpoint blockade benefit. Mu et al. demonstrated that FDG PET/CT radiomics predicted durable clinical benefit in advanced NSCLC treated with immune checkpoint blockade[15]. Similarly, Valentinuzzi et al[16] proposed an FDG PET immunotherapy radiomics signature to predict response to pembrolizumab. Compared with high-dimensional radiomics, gETU and NHOC/NHOP offer simpler, more interpretable features; however, our results suggest that hotspot location metrics may require refined definitions (e.g., lesion wise vs patient level aggregation, multilesion weighting, or

incorporation into radiomics signatures) to yield robust incremental prediction in chemo-immunotherapy cohorts.

From a clinical decision making standpoint, the incremental benefit of adding gETU to a baseline clinical+molecular model was supported by decision curve analysis, a method designed to quantify net benefit across threshold probabilities relevant to clinical action[17]. Our cross-validated discrimination analysis also aligns with recommended practices for internal validation of prognostic models in survival settings, emphasizing out of sample evaluation to reduce optimism[18].

Limitations of the study

This study has several limitations. First, stage distribution was skewed toward advanced disease, reflecting regional referral patterns where patients typically present only after experiencing significant symptoms. As a result, stage I–II counts were small, limiting generalizability and necessitating ridge-regularized sensitivity analyses. Second, gETU was nearly collinear with TLG and MTV, indicating that in this dataset it largely functioned as a tumor burden surrogate rather than a distinct heterogeneity marker. Third, PD-L1 category was not independently prognostic, which may relate to the chemo-immunotherapy treatment context across PD-L1 strata and known spatial heterogeneity of PD-L1 expression. Fourth, decision curve analysis was exploratory and should be interpreted cautiously given the retrospective design. Despite these limitations, strengths include the unified evaluation of hotspot weighted uptake, hotspot spatial descriptors, standard PET burden metrics, and molecular biomarkers, with internal validation and net-benefit assessment to contextualize clinical utility.

Conclusion

In NSCLC patients receiving first-line chemo-immunotherapy, hotspot weighted uptake (gETU) was independently associated with OS and PFS and provided incremental predictive value beyond TNM stage and molecular biomarkers. Hotspot location descriptors (NHOCmax/NHOPmax) did not consistently add prognostic value once metastatic stage and metabolic burden were considered. Prospective multi-center validation and standardization of gETU implementation are warranted.

References

1. Sung H, Ferlay J, Siegel RL, Laversanne M, Soerjomataram I, Jemal A, Bray F. Global Cancer Statistics 2020: GLOBOCAN estimates of incidence and mortality worldwide for 36 cancers in 185 countries. CA Cancer J Clin. 2021;71(3):209-249. PMID: 33538338. doi:10.3322/caac.21660.

2. Gandhi L, Rodríguez-Abreu D, Gadgeel S, Esteban E, Felip E, De Angelis F, et al. Pembrolizumab plus chemotherapy in metastatic non-small-cell lung cancer. N Engl J Med. 2018;378(22):2078-2092. PMID: 29658856. doi:10.1056/NEJMoa1801005.

3. Paz-Ares L, Luft A, Vicente D, Tafreshi A, Gümüş M, Mazières J, et al. Pembrolizumab plus chemotherapy for squamous non-small-cell lung cancer. N Engl J Med. 2018;379(21):2040-2051. PMID: 30280635. doi:10.1056/NEJMoa1810865.

4. Haragan A, Field JK, Davies MPA, Escriu C, Gruver A, Gosney JR. Heterogeneity of PD-L1 expression in non-small cell lung cancer: implications for specimen sampling in

predicting treatment response. Lung Cancer. 2019;134:79-84. PMID: 31320000. doi:10.1016/j.lungcan.2019.06.005.

5. Boellaard R, Delgado-Bolton R, Oyen WJG, Giammarile F, Tatsch K, Eschner W, et al. FDG PET/CT: EANM procedure guidelines for tumourr imaging: version 2.0. Eur J Nucl Med Mol Imaging. 2015;42(2):328-354. PMID: 25452219. doi:10.1007/s00259-014-2961-x.

6. Chardin D, Paquet M, Schiappa R, Darcourt J, Bailleux C, Poudenx M, et al. Baseline metabolic tumor volume as a strong predictive and prognostic biomarker in patients with non-small cell lung cancer treated with PD1 inhibitors: a prospective study. J Immunother Cancer. 2020;8(2):e000645. PMID: 32709713. doi:10.1136/jitc-2020-000645.

7. Tricarico P, Chardin D, Martin N, Contu S, Hugonnet F, Otto J, Humbert O. Total metabolic tumor volume on 18F-FDG PET/CT is a game-changer for patients with metastatic lung cancer treated with immunotherapy. J Immunother Cancer. 2024;12(4):e007628. PMID: 38649279. doi:10.1136/jitc-2023-007628.

8. Yamaguchi O, Kaira K, Hashimoto K, Mouri A, Shiono A, Miura Y, et al. Tumor metabolic volume by 18F-FDG-PET as a prognostic predictor of first-line pembrolizumab for NSCLC patients with PD-L1 ≥50%. Sci Rep. 2020;10:14990. PMID: 32929123. doi:10.1038/s41598-020-71735-y.

9. Brose A, Miederer I, König J, Gkika E, Sahlmann J, Schimek-Jasch T, et al. Prognostic value of metabolic tumor volume on 18F-FDG PET/CT in addition to the TNM classification system of locally advanced non-small cell lung cancer. Cancer Imaging. 2024;24(1):171. PMID: 39709461. doi:10.1186/s40644-024-00811-7.

10. Rahmim A, Schmidtlein CR, Jackson A, Sheikhbahaei S, Marcus C, Ashrafinia S, et al. A novel metric for quantification of homogeneous and heterogeneous tumors in PET for enhanced clinical outcome prediction. Phys Med Biol. 2016;61(1):227-242. PMID: 26639024. doi:10.1088/0031-9155/61/1/227.

11. Hong S-P, Lee SM, Yoo ID, Lee JE, Han SW, Kim SY, Lee JW. Clinical value of SUVpeak-to-tumor centroid distance on FDG PET/CT for predicting neoadjuvant chemotherapy response in patients with breast cancer. Cancer Imaging. 2024;24(1):136. PMID: 39394156. doi:10.1186/s40644-024-00787-4.

12. Zheng C, Miao J, Xu L, Cai Y, Zheng B, Tan Z, Sun C. Novel PET imaging biomarkers as predictors of postoperative recurrence in lung adenocarcinoma. BMC Cancer. 2025;25(1):874. PMID: 40369441. doi:10.1186/s12885-025-14263-0.

13. Wasserthal J, Breit HC, Meyer MT, Pradella M, Hinck D, Sauter AW, et al. TotalSegmentator: Robust segmentation of 104 anatomic structures in CT images. Radiol Artif Intell. 2023;5(5):e230024. doi:10.1148/ryai.230024. PMID:37795137.

14. Isensee F, Jaeger PF, Kohl SAA, Petersen J, Maier-Hein KH. nnU-Net: A self-configuring method for deep learning-based biomedical image segmentation. Nat Methods. 2021;18(2):203-211. doi:10.1038/s41592-020-01008-z.

15. Mu W, Tunali I, Gray JE, Qi J, Schabath MB, Gillies RJ. Radiomics of 18F-FDG PET/CT images predicts clinical benefit of advanced NSCLC patients to checkpoint blockade immunotherapy. Eur J Nucl Med Mol Imaging. 2020;47(5):1168-1182. PMID: 31807885. doi:10.1007/s00259-019-04625-9.

16. Valentinuzzi D, Vrankar M, Boc N, Ahac V, Zupancic Z, Unk M, et al. [18F]FDG PET immunotherapy radiomics signature (iRADIOMICS) predicts response of non-small-cell lung cancer patients treated with pembrolizumab. Radiol Oncol. 2020;54(3):285-294. PMID: 32726293. doi:10.2478/raon-2020-0042.

17. Vickers AJ, Elkin EB. Decision curve analysis: a novel method for evaluating prediction models. Med Decis Making. 2006;26(6):565-574. PMID: 17099194. doi:10.1177/0272989X06295361.

18. Harrell FE Jr, Lee KL, Mark DB. Multivariable prognostic models: issues in developing models, evaluating assumptions and adequacy, and measuring and reducing errors. Stat Med. 1996;15(4):361-387. PMID: 8668867. doi:10.1002/(SICI)1097-0258(19960229)15:4<361::AID-SIM168>3.0.CO;2-4.

Characteristic	Value
Patients, n	149
Age, years	59 (53-65)
Sex, male	114 (76.5%)
TNM stage I	5 (3.4%)
TNM stage II	5 (3.4%)
TNM stage III	60 (40.3%)
TNM stage IV	79 (53%)
Histology: Adenocarcinoma	60 (40.3%)
Histology: Squamous Cell	52 (34.9%)
Histology: Other	37 (24.8%)
EGFR wildtype	106 (71.1%)
EGFR mutated	43 (28.9%)
PD-L1 negative	57 (38.3%)
PD-L1 low	47 (31.5%)
PD-L1 high	45 (30.2%)
SUVmax	14.30 (12.6-17.2)
MTV	65.70 (49.8-100.6)

TLG	502.1 (323.4-776.6)
gETU	537.60 (347.9-850)
NHOCmax	0.59 (0.49-0.74)
NHOPmax	0.39 (0.28-0.54)

Table 1. Baseline clinicopathologic and PET characteristics of the study cohort (n=149).

Variable	**HR**	**95% CI**	**P value**
Stage IV (vs I-III)	4.34	2.57-7.34	<0.001
EGFR mutated (vs wild type)	0.70	0.48-1.04	0.078
PD-L1 low (vs negative)	0.92	0.62-1.37	0.676
PD-L1 high (vs negative)	1.06	0.70-1.61	0.784
gETU (per 1 SD)	1.48	1.19-1.84	<0.001

Table 2. Multivariable Cox proportional hazards model for overall survival.

Variable	HR	95% CI	p
Stage IV (vs I-III)	46.19	18.08-118.01	<0.001
EGFR mutated (vs wildtype)	0.74	0.50-1.10	0.141
PD-L1 low (vs negative)	0.65	0.42-0.99	0.047
PD-L1 high (vs negative)	0.95	0.62-1.45	0.798
gETU (per 1 SD)	1.51	1.20-1.90	<0.001

Table 3. Multivariable Cox proportional hazards model for progression free survival.

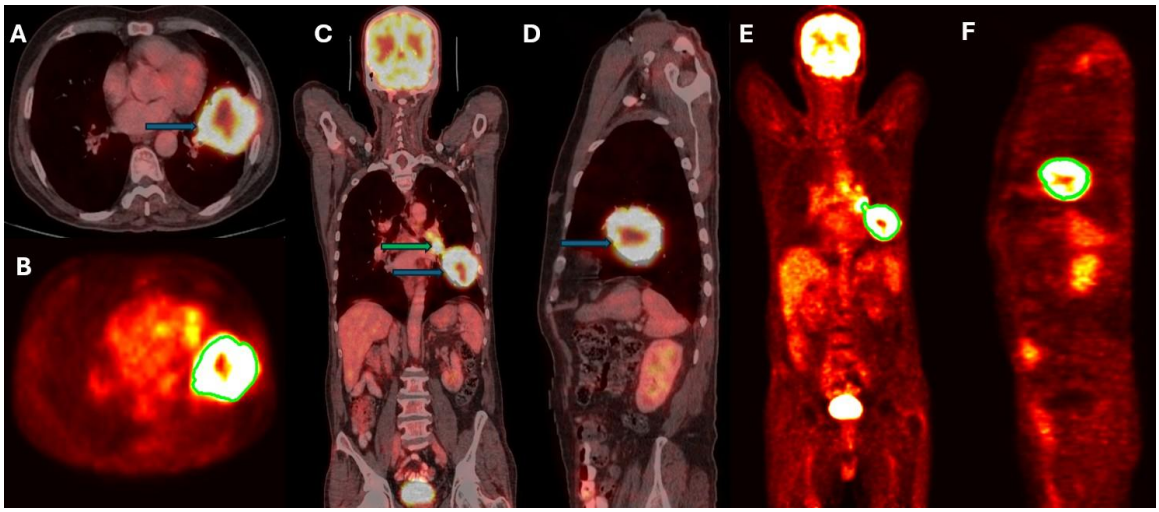


Figure 1. Multiplanar visualization of a hypermetabolic lung tumor and its segmentation on baseline ^{18}F-FDG PET/CT. **(A)** Axial fused PET/CT image demonstrates an intensely FDG avid peripheral lung mass (blue arrow). **(B)** Corresponding axial PET image shows the tumor segmentation, with the metabolically active tumor volume outlined by the **green contour**. **(C)** Coronal fused PET/CT image depicts the lesion in relation to adjacent thoracic structures, with arrows indicating the tumor (blue arrow) and a hilar lymph node (green arrow). **(D)** Sagittal fused PET/CT image further demonstrates the lesion extent in the anteroposterior dimension (blue arrow). **(E)** Coronal whole body PET projection image shows the segmented lung tumor outlined in green. **(F)** Sagittal PET projection image likewise demonstrates the segmented tumor volume with green ROI overlay. Together, these panels illustrate multiplanar anatomic metabolic depiction of the primary lung lesion and its PET based tumor segmentation for quantitative analysis.

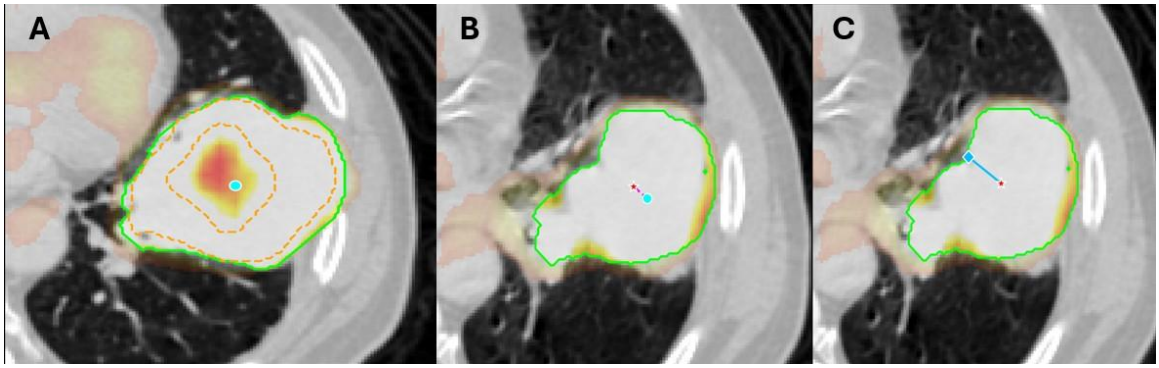


Figure 2. Visualization of gETU and hotspot spatial heterogeneity indices (NHOCmax and NHOPmax) in a lung tumor on baseline ^{18}F-FDG PET/CT**. (A)** Fused PET/CT axial image shows the tumor volume of interest (VOI) delineated by the green contour**.** The cyan marker indicates the intratumoral SUVmax voxel (hotspot) used as the reference point for spatial uptake weighting in the gETU framework. The orange dashed isocontours depict relative SUV isocontours referenced to SUVmax; the outer orange contour corresponds to the conventional metabolic tumor volume boundary defined by the 41% SUVmax threshold (MTV41)**,** whereas the inner contour represents a higher-uptake intralesional "core," illustrating uptake stratification and intratumoral

heterogeneity within the VOI. **(B)** Normalized hotspot to centroid distance **(**NHOCmax**)** is illustrated as the 3D Euclidean distance between the SUVmax voxel (cyan) and the tumor centroid (red star)**,** normalized to the equivalent sphere radius of the VOI (sphere with the same volume as the lesion), providing a size normalized measure of hotspot eccentricity. **(C)** Normalized hotspot to perimeter distance **(**NHOPmax**)** is shown as the minimum 3D distance from the SUVmax voxel (red star) to the closest point on the tumor boundary (blue diamond) (blue line), likewise normalized to the equivalent-sphere radius, quantifying the peripheral proximity of maximal FDG uptake.

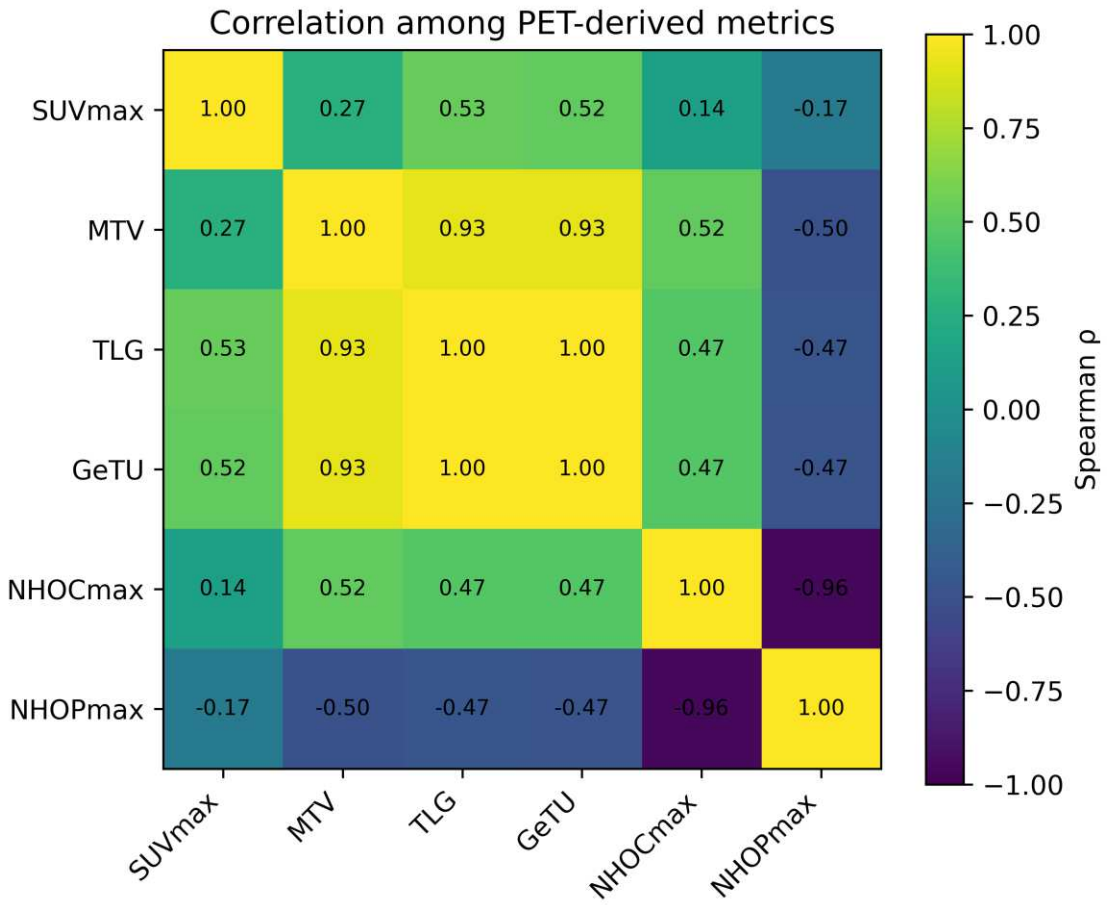


Figure 3. Correlation heatmap of PET-derived metrics. Spearman correlation coefficients (ρ) among SUVmax, MTV, TLG, gETU, NHOCmax and NHOPmax are shown for the full cohort (n =149). Values are annotated within cells.

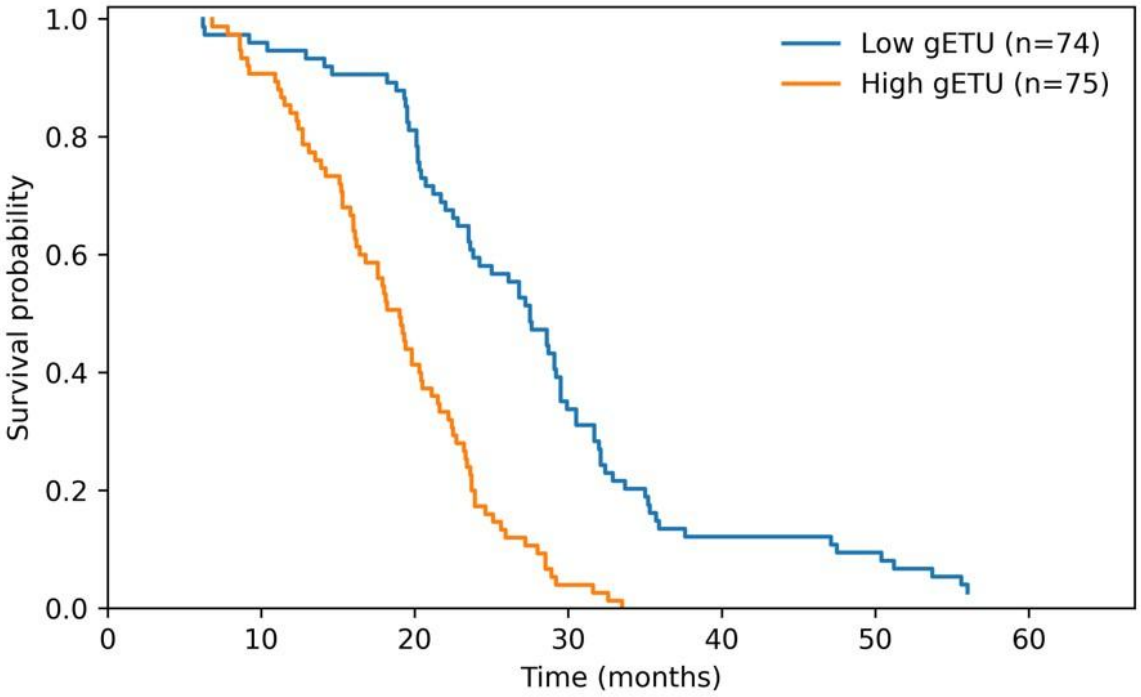


Figure 4. Kaplan-Meier overall survival by baseline gETU. Patients were dichotomized by median gETU. Survival curves are compared using the log-rank test.

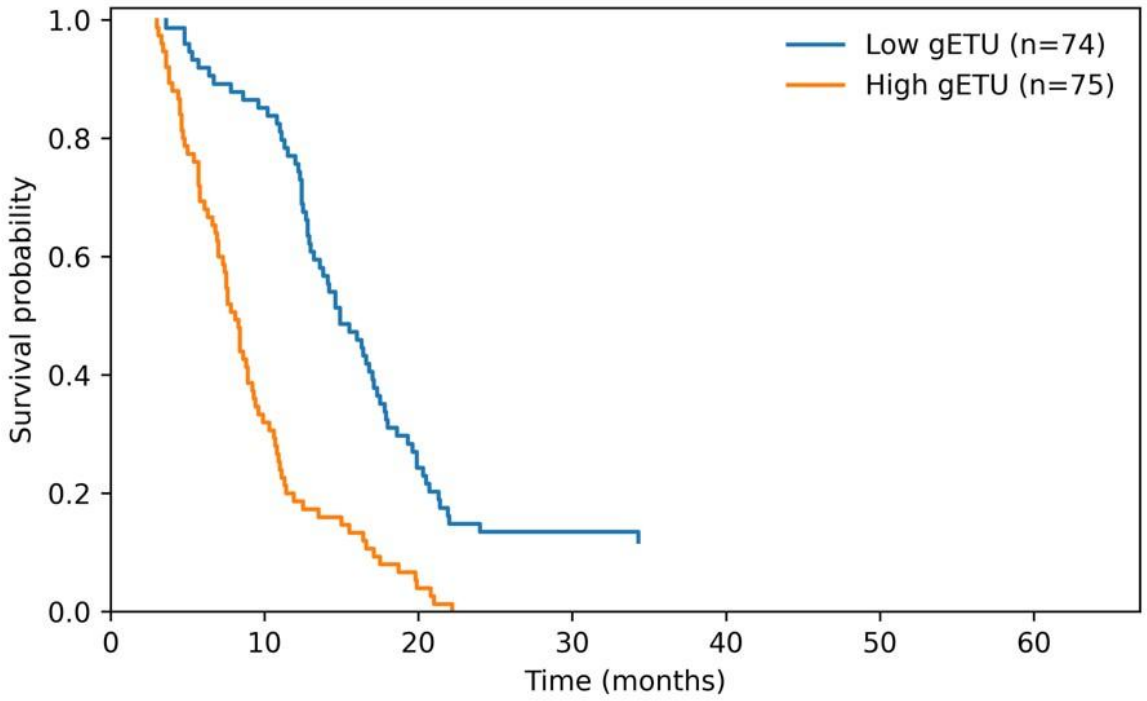


Figure 5. Kaplan-Meier progression free survival by baseline gETU. Patients were dichotomized by median gETU. Survival curves are compared using the log-rank test.

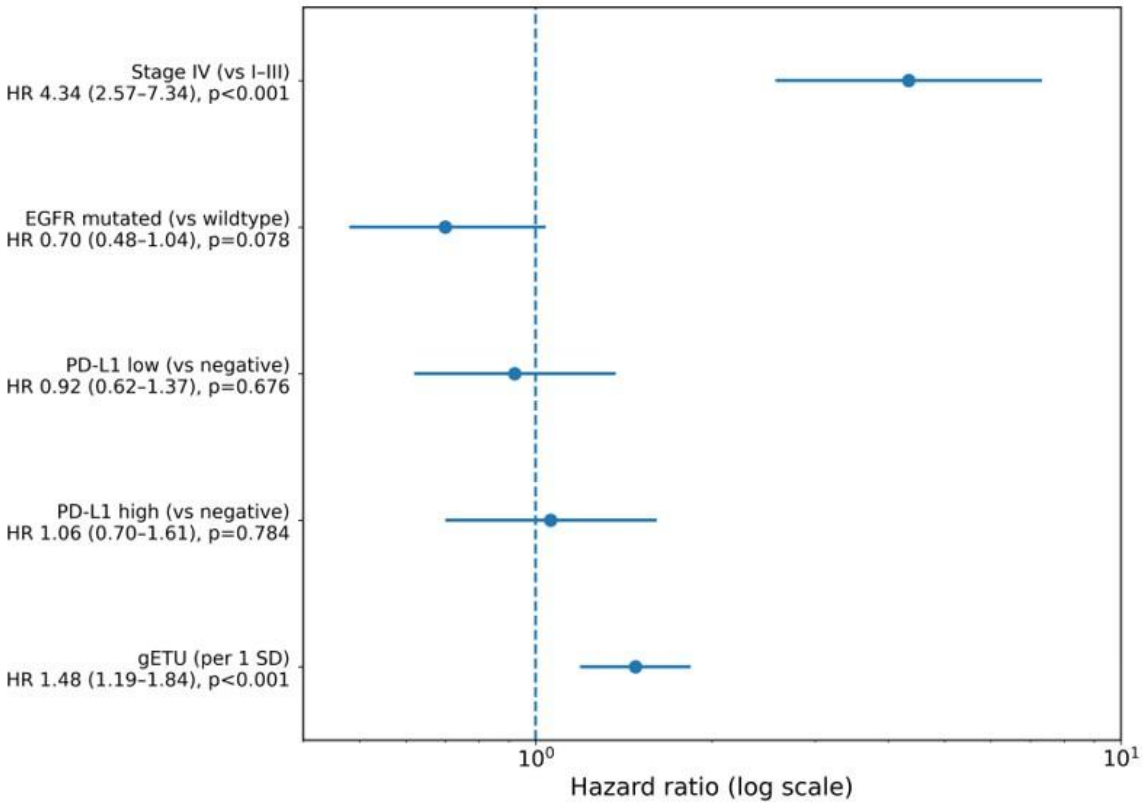


Figure 6. Multivariable Cox model for overall survival. Forest plot shows hazard ratios and 95% confidence intervals for stage IV (vs I-III), EGFR mutation, PD-L1 categories (vs negative), and gETU (per 1 SD).

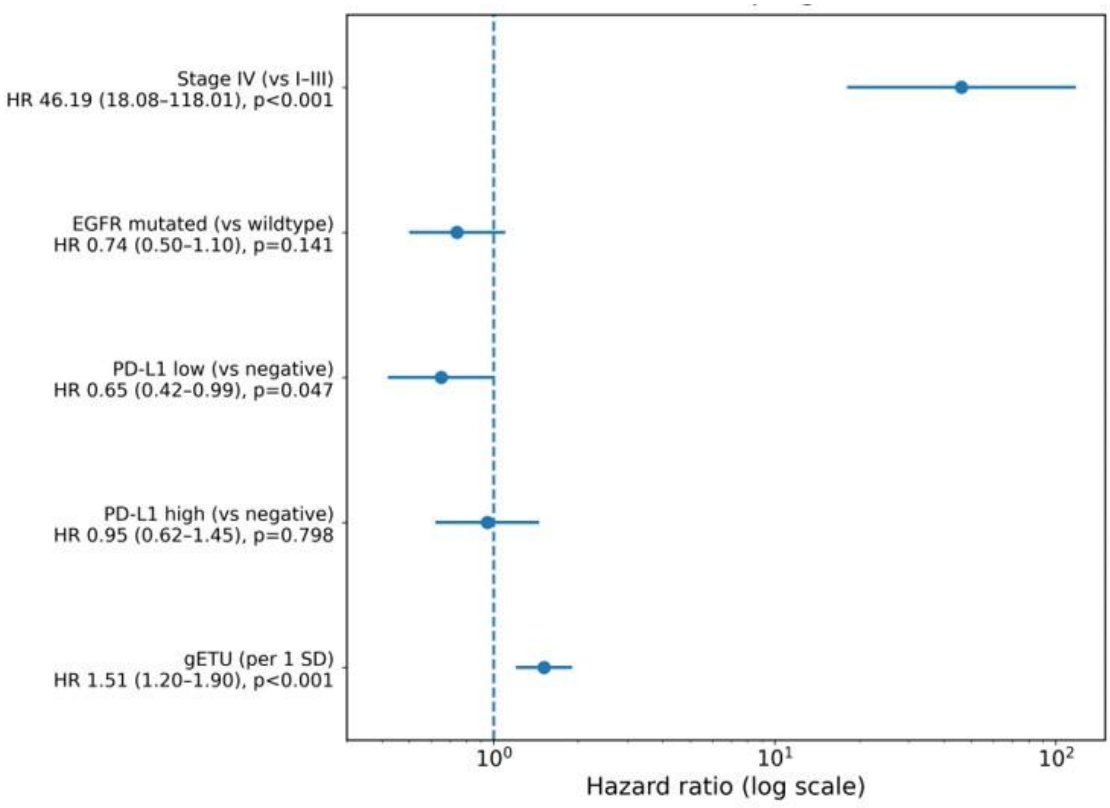


Figure 7. Multivariable Cox model for progression free survival. Forest plot shows hazard ratios and 95% confidence intervals for stage IV (vs I-III), EGFR mutation, PD-L1 categories (vs negative), and gETU (per 1 SD).

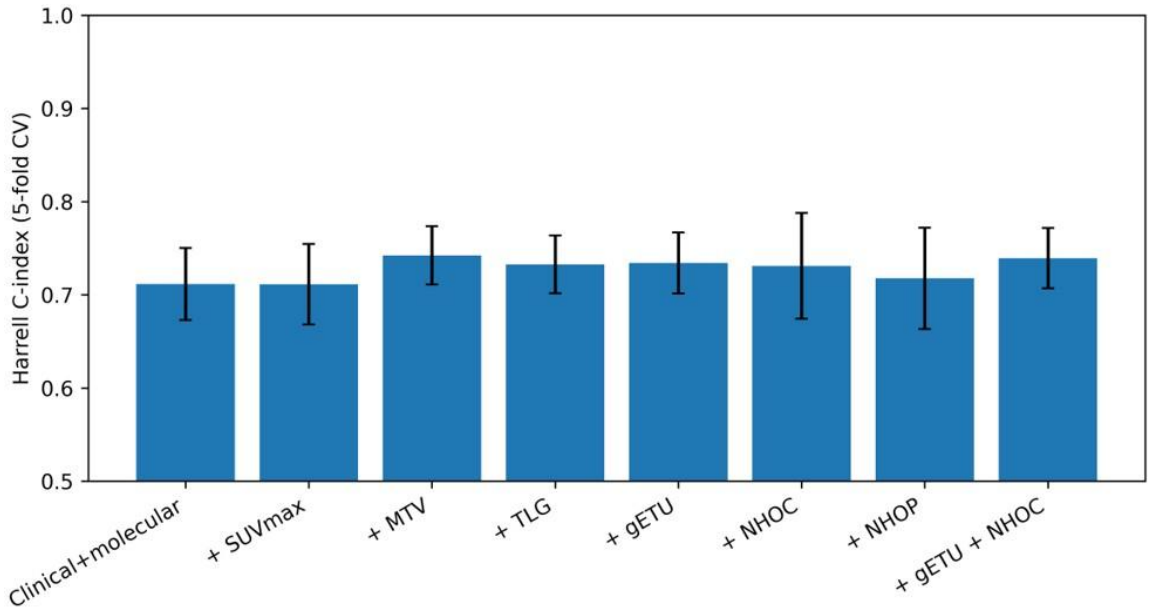


Figure 8. Cross validated discrimination for overall survival models. Bars show mean 5 fold cross validated Harrell C-index with standard deviation. The baseline clinical and molecular model includes age, sex, histology, stage IV (vs I-III), EGFR and PD-L1; PET features were added as indicated.

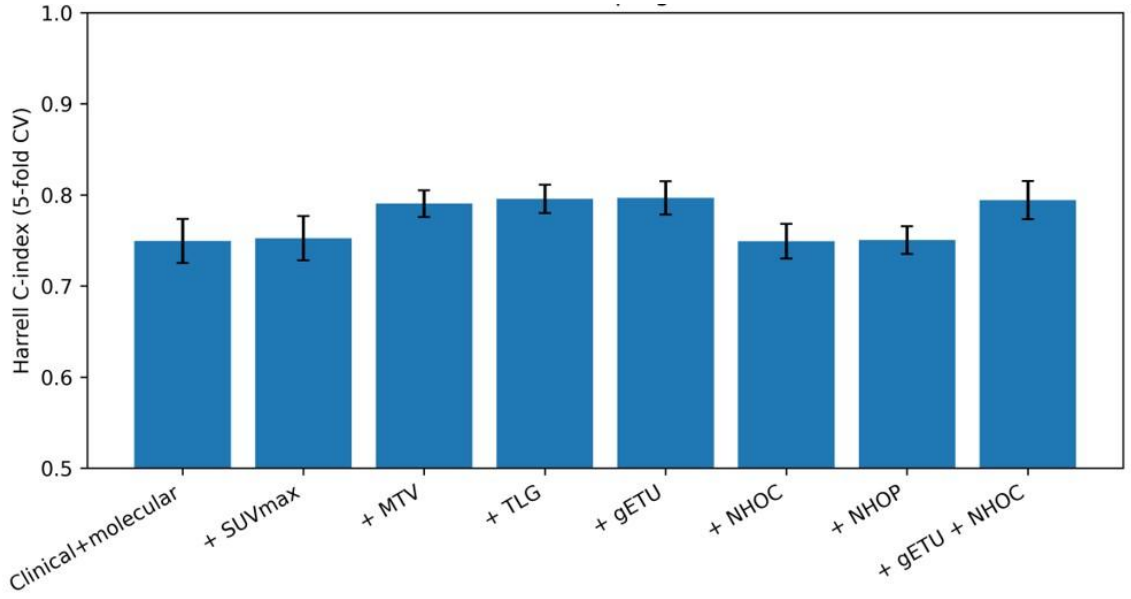


Figure 9. Cross validated discrimination for progression free survival models. Bars show mean 5 fold cross validated Harrell C-index with standard deviation. The baseline clinical+molecular model includes age, sex, histology, stage IV (vs I-III), EGFR and PD-L1; PET features were added as indicated.

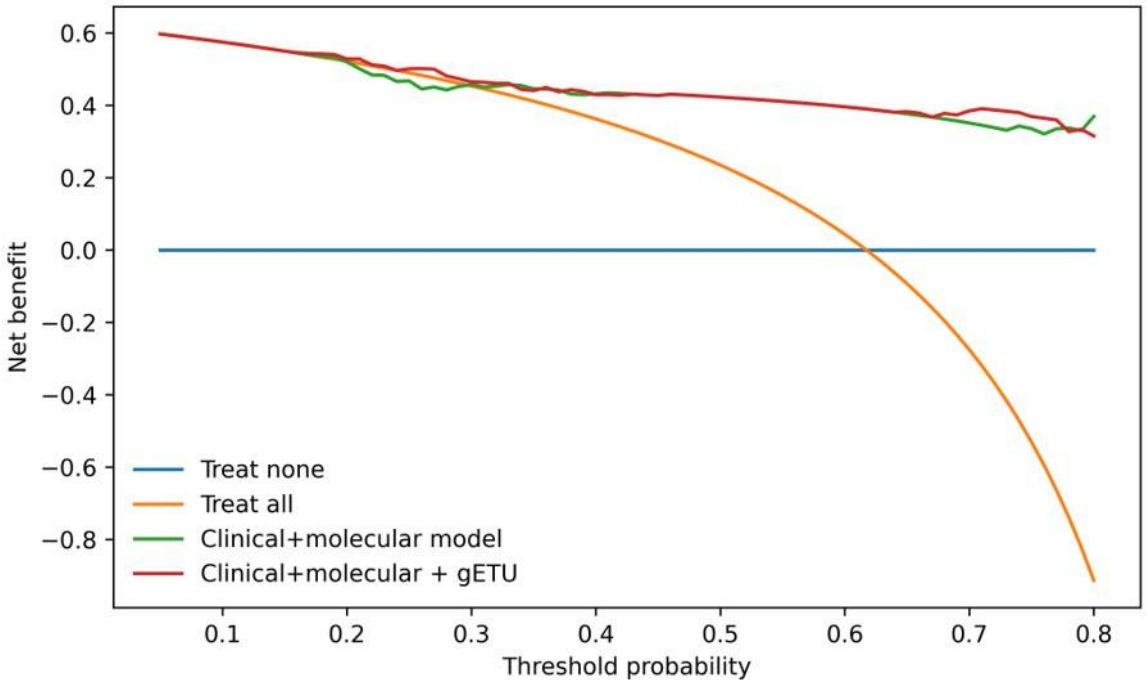


Figure 10. Decision curve analysis for 24 month overall survival risk. Net benefit is shown for the baseline clinical+molecular model and the gETU augmented model across threshold probabilities. 'Treat all' and 'treat none' strategies are included for reference.

Supplementary Files

This is a list of supplementary files associated with this preprint. Click to download.

- SupplementaryTableS1A.docx
- SupplementaryTableS1B.docx